

Fikeraddis Elias Lemma



# Knee Angle Measurement for Knee Implants

Helsinki Metropolia University of Applied Sciences

Bachelor of Engineering

Electronics

Thesis

October 2015

Author(s)	Fikeraddis Lemma
Title	Knee Angle Measurement
Number of Pages	37 pages + 8 appendices
Date	06 October 2015
Degree	Bachelor of Engineering
Degree Programme	Electronics
Instructor	Drs.Ing. Patrick Pelgrims (Project Manager) Matti Fischer , Principal Lecturer (Project Manager)
<p>The Knee angle project was carried out at Thomas More University in Belgium. The aim of the project was to measure the change in rotational angle of the knee prosthesis and create a stable data reading between sensors, ADC (analog digital converter), microcontroller and a wireless module. In addition, the project was aimed at presenting readable and understandable code flow with a development of better performance. The Knee measurement system for knee implant reduces knee replacement complications and expenses. Also, it provides closer control and visualization of knee prosthesis so that it will be easy to improve patient health. The thesis explains the devices and methods used in this project.</p> <p>The development of the knee angle measurement system comprised of four parts; Analog front end, sensor part, microcontroller and wireless module. Hardware devices and software applications were used in testing and analyzing the results, for example- Saleae logic analyzer, USB to UART converter and LabVIEW.</p> <p>The project showed the expected result with complete functionality of the wireless module and the sensor with a stable change in amplitude. The analog to digital converter had minor SPI timing problems that can be solved by a closer study of the timing properties of SPI in the ADS.</p>	
Keywords	Human Joint, ADS1296,nRF24L01, Microcontroller, SPI, Sensors

## **Contents**

### **1 Introduction**

### **2 Human Knee Joint**

#### 2.1 Knee Arthritis

##### 2.1.1 Rheumatoid Arthritis

##### 2.1.2 Osteoarthritis

#### 2.2 Knee Replacement (Arthroplasty)

### **3 Theoretical Backgrounds of the System**

### **4 Components Used In Knee Angle Measurement System**

#### 4.1 Magnet S-05-08-N

#### 4.2 Sensor Units: AMR Sensor Principle

##### 4.2.1 HMC1512

##### 4.2.2 LIS3MDL Digital Sensor

##### 4.2.3 LIS3MDL Adapter Board (STEVAL-MKI137V1)

#### 4.3 Analog Front End

##### 4.3.1 ADS1296

##### 4.3.2 Operation Principle

##### 4.3.3 Interfacing ADS1296

#### 4.4 Microcontroller: MSP430

##### 4.4.1 Operation Principles and Mode

##### 4.4.2 Clock System

##### 4.4.3 Enhanced Universal Serial Communication Interface-SPI Mode

##### 4.4.4 MSP-FET430UIF Universal Programmer

#### 4.5 Wireless Module: nRF24L01

##### 4.5.1 Hardware Features

##### 4.5.2 Interfacing the nRF24L01

##### 4.5.3 Transmitter and Receiver

## **5 Comparison of the System**

5.1 Hardware and Software

5.2 Power Consumption

## **6 Testing Devices and Results of the System**

6.1 Saleae Logic Analyzer

6.2 MCP2200 (USB 2.0 to UART Protocol Converter with GPIO)

6.2.1 Real Term

6.3 LabVIEW

## **7 Conclusions and Discussion**

References

Appendices

Appendix 1. Measurements set up including Transmitter and Receiver ends

Appendix 2. QFN24 Package design for the Microcontroller

Appendix 3. Saleae Logic Analyzer test results

Appendix 4.1 Four different magnet position setups

Appendix 4. 2 Four different magnet position setups

Appendix 4.3 Magnetic data taken at 4 GAUSS for 12 samples

Appendix 4.4 Graphical representation of the four setups in XYZ

Appendix 5. Test result in LabVIEW development software

## Acronyms

<b>AFE</b>	Analog Front End
<b>ASIC</b>	Application Specific Integrated Circuit
<b>ADC</b>	Analog Digital Converter
<b>AMR</b>	Anisotropic Magnet Resistance
<b>ULP</b>	Ultralow Power
<b>MCU</b>	Microcontroller
<b>SPI</b>	Serial Peripheral Interface
<b>GND</b>	Ground
<b>I2C</b>	Inter Integrated Circuit
<b>PE</b>	Polyethylene Insert
<b>PGA</b>	Programmable Gate Amplifiers
<b>FP</b>	Femoral Part
<b>TP</b>	Tibial Part
<b>LPM</b>	Low Power Mode
<b>eUSCI</b>	Enhanced Universal Serial Communication Interface

## 1 Introduction

Knee angle Measurement started at Thomas More University with the collaboration of EmSys group that aim in development and implementation of embedded systems. The project was started between two students from Thomas More University (Kevin Sebrechts and Sven Sleenckx) and continued in improving the system.

This project is a part of a knee angle measurement system project for artificial knee implants, consisting of a Knee Unit: an in vivo system which would be part of knee implants; A Data Logger: an outside system used to receive data wirelessly from the Knee Unit; and an outside power supply unit which would supply power wirelessly to the in vivo Knee Unit.

The target system for this project is the in vivo Knee Unit which consists of different peripheral units such as: a sensor unit (HMC1512), analog front end (AFE) ADS1296, a microcontroller (MSP430FR5724) unit and a wireless communication module (nRF24L01).

The main focus of this paper is the explanation of a C software code which was modified according to a new version of printed circuit board for the Knee Unit. Power efficiency is an essential part of the entire scheme since the plan is to use an outside vivo wireless inductive power supply unit in the future. In the new version of the code various programming techniques were used to save power resulting in a more energy efficient system. These measures include: changing the software SPI communication used in the previous software to hardware peripheral SPI; using interrupts to enter to low power mode and sleep the processor; and taking advantage of the ULP(Ultra low power) advisor of code composer studio for modifying the code accordingly. After the communication; the project continued with adopting a new sensor (LIS3MDL) in reducing the size of our PCB.

## 2 Human Knee Joint

The knee is a joint formed to sustain and move bones, ligaments and tendons. It is the largest joint in the human body and formed by the assertion of a femur in the upper part of knee and tibia in the lower leg.

The knee joint shown below in figure 1 is one of the important and strongest parts of human body. It supports human body weight and allows movement of the lower leg relative to our thigh. Our day to day activities, including running, walking, standing and sitting depend on this joint.



Figure 1. Human Knee Joint (Copied from Cape Town knee surgery [1]).

Femur - is the strongest and heaviest bone that supports the entire human body. Our body weight is supported by femur while doing different activities such as running, sitting, walking and jumping.

Tibia (Shinbone) – is the stronger and larger one of the two lower leg bones. Lower leg and foot muscles are anchored to the tibia. In the same manner, it is essential for supporting body weight and various movement activities; such as running, jumping, sitting and walking.

Fibula – is the long, thin and lateral bone of the lower leg. Fibula supports lower leg muscles and helps in stabilizing an ankle. Because of its thin size, its function relays on supporting tibia.

Tibia, femur and fibula are closed with articular cartilage, which is an elastic material that act as shock absorber and grant our knee to move calmly. This pivotal joint is immersed in synovial fluid and allows six-degree of freedom motion. Figure 2 shows knee joint rotation in three anatomical planes and translation in three anatomical planes

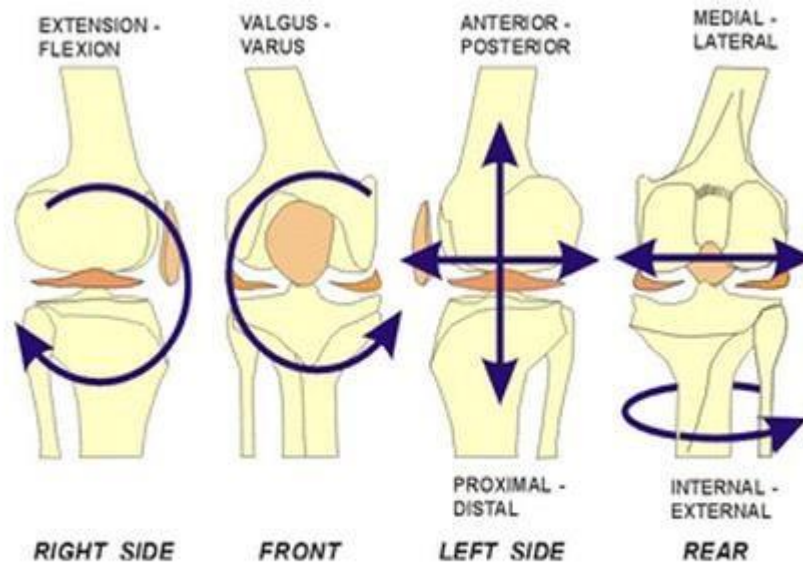


Figure 2. Knee movement anatomical planes (Copied from Tom's Physiotherapy Blog [2]).

The triangular shaped bone on the front side of knee that protects the knee joint is called Patella (knee cap). The Human knee joint can face enormous knee joint problems due to different reasons.

## 2.1 Knee Arthritis

Musculoskeletal (Rheumatic) diseases consist of over 150 diseases categorized under Joint diseases, physical disability, spinal disorder and conditions happening from trauma.

These musculoskeletal diseases cause a high rate of disability and risk of a proper functioning of day to day activities that affect personal life. The common knee joint diseases are listed and discussed below.



### 2.1.1 Rheumatoid Arthritis

Arthritis is one of the known diseases that affect joints, connective tissues, fibrous tissue, muscles and tendons which occur during early childhood. It causes disability and deformity of joints. It is commonly visible in women in developed countries with a rate varying between 0.3 % and 1 %.

### 2.1.2 Osteoarthritis

Degenerative joint disease is another name for osteoarthritis that creates a breakdown of articular cartilages. It mostly happens in old people and comes as a consequence of aging. Force resistant joints face osteoarthritis including hips, knees, fingers and lower spine regions. The data from world health organization states osteoarthritis as one of the most disabling diseases worldwide with an estimation rate of 9.6 % of men and 18.0 % of women aged above 60 years showing significant osteoarthritis.

## 2.2 Knee Replacement (Arthroplasty)

The knee joint is exposed to a developmental joint disease and injuries due to workload and shocks. In order to help injuries and developmental disorders, knee replacement should be carried.

Knee replacement (knee arthroplasty) is a surgical procedure carried out to replace fully or partially the weight bearing part of the knee with prosthetic part (artificial leg).

Knee Prosthesis consists of a femoral part, a tibia part and polyethylene which is inserted between the femoral and tibia part. The procedure differs depending on the fixation, material and design. An extra careful procedure is needed in knee prosthesis procedures; misalignment, ligament imbalance, loosening and a problem in the polyethylene causes an adverse effect on the replacement.

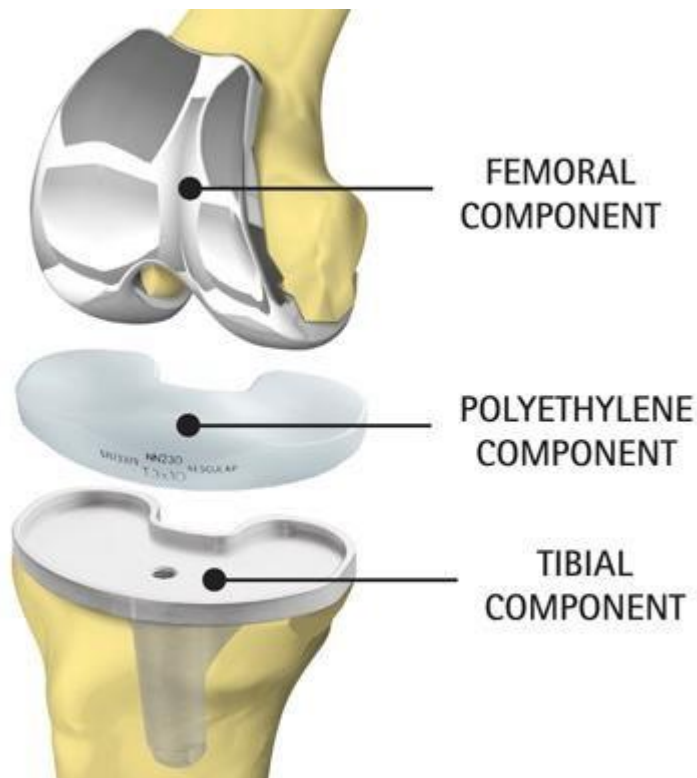


Figure 3. Knee Prosthesis design (Copied from AESCULAP Implant Systems [3])

In knee prosthesis femur and tibia are the most important joints in knee joint. Figure 3 shows knee replacement design with femoral part attached to the lower end of femur and the tibial component attached to the top end of tibia to hold the PE component.

Figure 4 below describes the upper and lower part of knee prosthesis metal parts. The upper part of the prosthesis has a metal curved around the Femur, the lower part consists of PE (polyethylene insert) to be placed between the femur and tibia to help as a cartilage and another metal part to be secured to the tibia.



Figure 4. The above figure shows Knee prosthesis descriptions and F.I.R.S.T.knee prosthesis by Symbios Orthopédie SA (Copied from Arash Arami (2014) [5, 95]).

There are two types of knee replacements

- Total knee replacement that includes both (left and right) sides of knee replacement.
- Partial knee replacement is where only one side of the knee is damaged or diseased and need a knee replacement.

Artificial prosthesis relieves patient pain and allows better movement of the knee. A study shows that more than 60,000 knee replacement surgeries are held in the USA and over 70,000 in England and Wales. This often occurs on aged people over 65 years.

Total knee replacement is a more complex procedure than partial knee replacement and these procedures require precise measurements and removal of the damaged or diseased part of the bones. The artificial knee is implanted by building each component at a time to free complexity.

### 3 Theoretical Backgrounds of the System

As explained in the introduction section, this project focused on a knee angle measurement in an artificial leg. Figure 5 shows different system integrations used while working on the knee angle measurement project: Linear/Angular/Rotational displacement sensors (HMC1512), low power 8 channel 24 bit analog front-end ADS1296, MSP430F57xx family mixed signal microcontroller (MSP4305724) and nRF24L01+ single chip Transceiver. The operation principle of the whole system is explained step by step as follows.

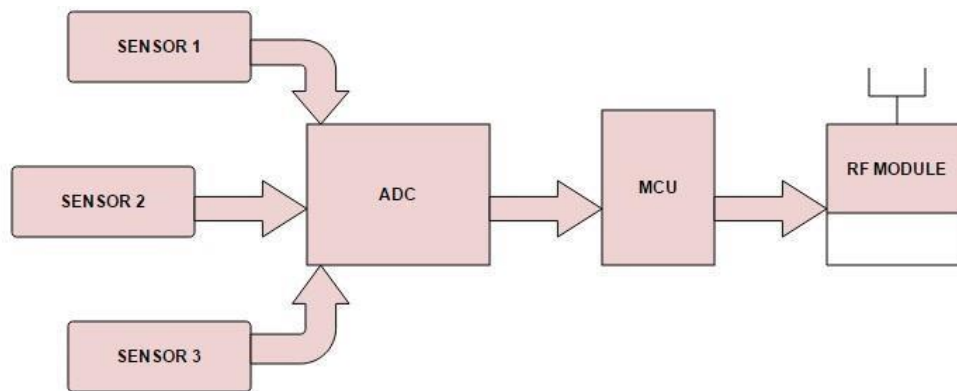


Figure 5. Block diagram of the system

At first the magneto-resistive sensors sense the strength of the magnetic field which varies relative to the position of the magnet in reference to the sensors. Then this data collected by the sensors is fed to the ADS for amplification and ADC conversion. After conversion, the analog data received from the sensors is presented in a 24 bit format and is fed to the MSP microcontroller via SPI bus.

Afterwards, the 24 bit data from the analog front end is modified by the microcontroller to 16 bit format and is sent to the wireless module (nRF24L01+) via SPI bus for wireless transmission. The Knee angle measurement project continues in replacing HMC1512 magnetic displacement sensor by LIS3MDL digital sensor.

The communication of the sensors to AFE (analog front end) has been configured in SPI interface has been used while replacing the new sensor (LIS3MDI) to communicate with MSP430. The position of the sensors is an important aspect of getting proper data reading.

Figure 6 shows the rotation of knee joint and position of the three sensors. The sensor attachment position has a direct effect on the measurement accuracy so extra careful procedures should be taken.

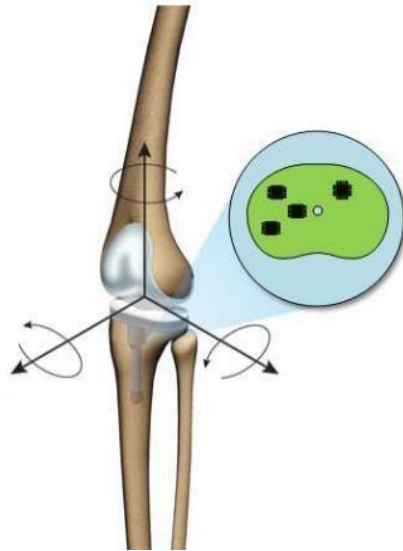


Figure 6. Sensor positioning in human knee joint (Copied from Knee angle measurement thesis documentation [4]).

The sensor is positioned in the polyethylene insert (plastic) part of the replacement and the magnet in the femoral part of the human knee joint.

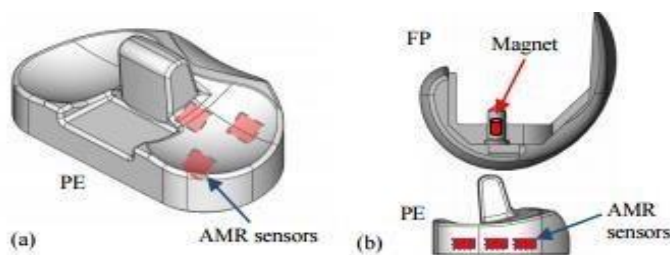


Figure 7. (a) AMR sensor inside PE. (b) Magnet in FP and AMR sensor position (Copied from Arash Arami (2014) [5, 95]).

Figure 7 above implies position of the magnet and the three sensors. The magnet is situated in the femoral part and the sensors on the PCB situated on the PE (Polyethylene Insert).

## 4 Components Used In Knee Angle Measurement System

Various unit systems have been used while working on knee angle measurement project.

1. Magnet
2. Sensor Unit
3. Analog Front End
4. Microcontroller
5. Wireless Module

This section discusses these system units in brief and appendix 1 shows the measurement setup together with receiver and transmitter part of the wireless module

### 4.1 Magnet: S-05-08-N

The S-05-08-N is a very small magnet with a diameter of 5 mm and height of 8.47 mm. This strong rod magnet has magnetization level of N45 in which the letter "N" indicate the maximum working temperature of the magnet in this case 80 °C and the number indicating the maximum energy product of the magnet.

The maximum amount of magnetic energy stored in a magnet can be measured to detect the maximum energy product of a magnet with a unit of  $\text{kJ/m}^3$  or MGOe (MegaGauss-Oersted). Considering S-05-08-N, it has a magnetization of N45 telling a maximum temperature of 80 °C with energy product level of 45  $\text{kJ/m}^3$  or 358 MGOe.

### 4.2 Sensor Unit: AMR sensors principle

AMR sensors have Si or glass board and a thin film of ferromagnetic metals (like Ni and Fe) on the board. Figure 8 below shows decrease in resistance with the strength of magnetic field when current (I) is applied to the ferromagnetic thin film metal in the direction of Y and magnetic field (H) to the direction of X that is vertical to the current direction.

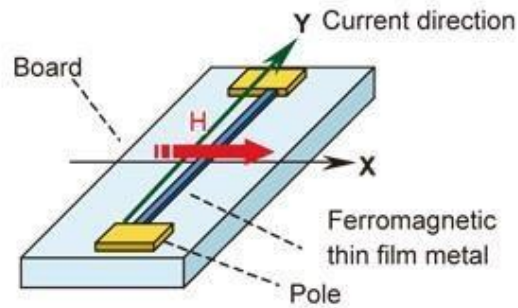


Figure 8. AMR sensors (Copied from KOHDEN [12]).

#### 4.2.1 Linear/Angular/Rotary Displacement Sensor

Honeywell's HMC1512 is a high resolution, low power sensor with the ability of measuring the angle direction of a magnetic field from a magnet with a wide angular range of  $\pm 90^\circ$  with  $< 0.05$  resolution and can give full scale output ranges of 120 mV with 5V of power supply.

It follows AMR sensing principle which changes the value of the magnetic resistance according to the strength of the magnetic field.

Figure 9 shows the sensor in the form of Wheatstone bridge that measure magnetic field direction.  $R$  (resistor) of the four resistors has the same value and the power supply ( $V_s$ ) sources current to flow through the resistors in the direction as shown below in figure 9 for each resistor.

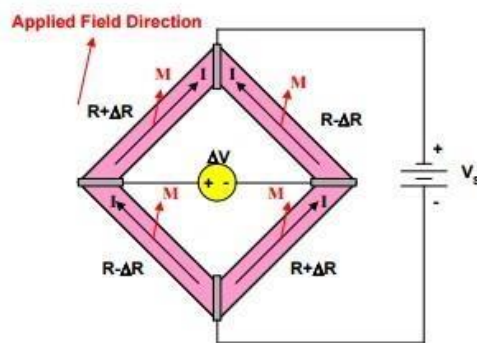


Figure 9. Basic sensor bridge schematics (Copied from Honeywell [13]).

The system consists of three HMC1512 magnetic sensors aligned in T shape to detect the relative angle of the magnet to a different axis. The human knee can move in three different axes, thus we should also be able to measure this angle relative to those.

#### 4.2.2 LIS3MDL Digital Output Magnetic Sensor

The project continues with a plan of replacing the sensor with an ultra-low power, high performance 3-axis magnetometer; LIS3MDL. It has the same working principle, three sensors and analog to digital converter with a central unit microcontroller in communication with a wireless module (nRF24L01).

LIS3MDL is a 16-bit data output sensor with a wide supply voltage of 1.9 - 3.6 v range. It has selectable magnetic full scale allowing selectable conversion mode for better performance. It can be configured in SPI or I2C mode depending on user selection moreover, it allows self-test for a proper operation of the sensor.

LIS3MDL sensor is preferable due to its advantage in allowing selectable test conditions for sensitivity test, wide supply voltage range and easy device identification by configuring the WHO\_AM\_I register for self-test.

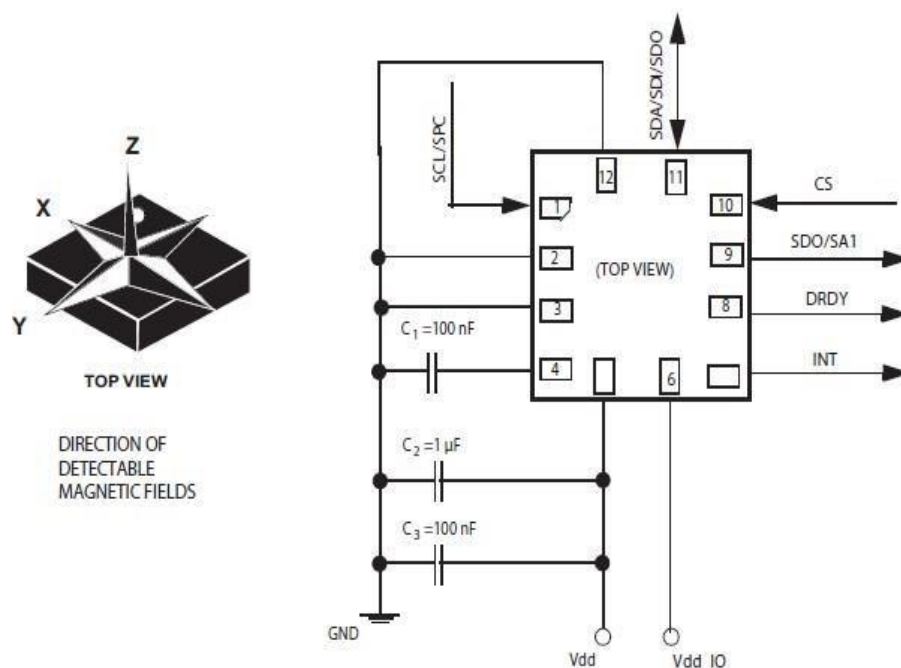


Figure 10. Showing electrical connections of LIS3MDL (Copied from STMicroelectronics datasheet [14]).



External capacitors are needed for proper functioning of the sensor; as shown from figure 10 schematic. It is possible to solder the external capacitor as stated, but there is a readymade adapter board with all the necessary features.

The configuration of LIS3MDL is important for proper functioning of the sensor. The control registers should be set to use the features. Mainly CTRL\_REG1, CTRL\_REG2, CTRL\_REG3, CTRL\_REG4 and CTRL\_REG5 should be used. LIS3MDL allows both SPI and I2C configuration with different pin descriptions. The I2C interface only acquires two signal lines, a serial clock line and a data line. In addition to the pins, there are other necessary modes and requirement to fulfill. In this paper, only SPI interface will be discussed.

The control registers have specific applications. CTRL\_REG1 allows configuring the operational mode and output data rate with different frequency values according to usage. Enabling the FAST ODR (output data rate) from this register is important in selecting the proper ODR (output data rate) and OM (operational mode). The data rate configuration depends on the output data rate and on the FAST output data rate selection with operational mode preferences (low power, medium power, high power and ultrahigh power) which is stated on the datasheet of the sensor. Focusing on Low power was an important aspect but due to the frequency requirement, the needed ODR (operational data rate in Hz) shifted to UHP with an ODR of 155.

To adjust the measured input dynamic range of the device to the amplitude of the magnetic field, configuring CTRL\_REG2 is a must. The LIS3MDL sensor allows variant choices with gain at 16-bit. All the full-scale selections were taken to visualize the performance of the sensor.

Table 1. Full scale selections: FS0 (full scale selection zero) and FS1 (full scale selection one) (Copied from STMicroelectronics Datasheet [15, 7])

FS1	FS0	Full-scale [G]	Gain@16-bit (LSB/G)
0	0	±4	6842
0	1	±8	3421
1	0	±12	2281
1	1	±16	1711

Table 1 states two full-scale selections cases FS1 (full scale selection one) and FS0 (full scale selection zero) with gauss and gain values.

This helps to evaluate the input dynamic state of the device to the amplitude of the magnetic field to be measured. In this project all full scale levels were tested to visualize the magnetic field of the magnet. The system mode runs in continuous measurement of data and writes the measured data in specific data output registers for a read. The data read has been configured using the STATUS\_REG to examine the lower and higher end of the three axes (X, Y and Z).

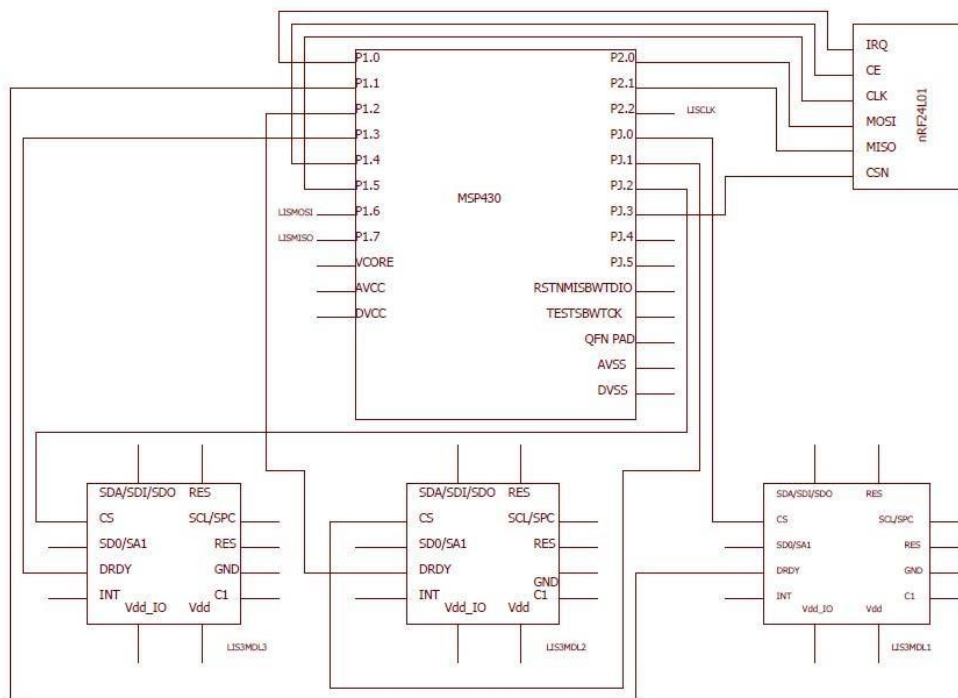


Figure 11. Schematic design of LIS3MDL sensor to MSP430 and nRF24L01

Using Eagle, the above figure 11 was designed showing the connection from the LIS3MDL to MSP430 and nRF24L01. MSP430FR5724 microcontroller was used in connection between the sensors and wireless module. The design is based on the datasheet of the devices and used pin description. As mentioned above, both I2C and SPI interface can be used to interface LIS3MDL and both of these configurations have been tried in this project due to acknowledgment bit responsiveness of the Master (MSP430) in SPI.

Focusing on SPI, It can be achieved through four wires, CS, SCL, SDO and SDI. CS is the serial enable port that goes low at the start of transmission and back to high at the end. SCL is the serial clock which is controlled by the Master. SDI and SDO are the serial data input and output ports.

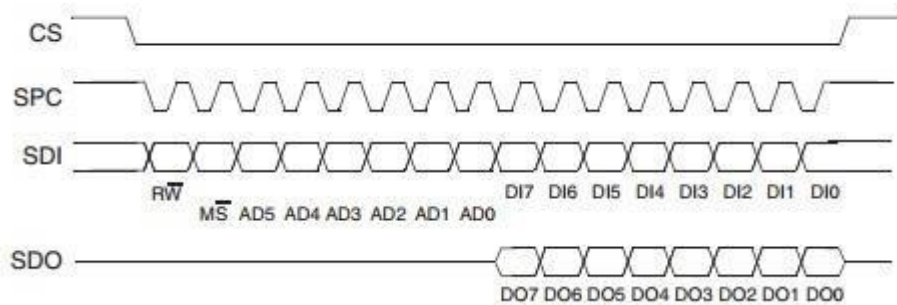


Figure 12. Read and write protocol of LIS3MDI in SPI (Copied from STMicroelectronics datasheet [14]).

The above figure 12 describes the data read and writes protocol for SPI interface. The SPI read and write command is carried out with 16 bit clock pulses.

The RW bit (bit 0) indicates two conditions when RW is 0, data is written into the device that is DI (7:0). On the other hand when 1, data is read from the device DO (7:0). MS bit also has two possible cases when 0, it indicates the address stays unchanged in multiple read/write commands and when 1, the addresses will be auto incremented in multiple read/write. The AD (5:0) shows the address of the registers. Due to lack of information on the sensor functionality and configuration in SPI, I2C interface has been tried to check the normal functionality of the LIS3MDL.

There are four important terms to understand the functionality of the sensor in I2C interface. Transmitter; the device that send data to the bus, Receiver; the device that receives data from the bus, Master; the device responsible to initiate the transfer, generate clock signal and also halt the transfer and lastly, Slave; which can be addressed by the master. LIS3MDL provides self-test features in order to test the sensor by enabling the test bit of CTRL\_REG1 and also consists of temperature sensor suitable in temperature measurement in the same control register.

### 4.2.3 LIS3MDL adapter board (STEVAL-MKI137V1)

The adapter board is used for better usage and functionality of the LIS3MDL sensor. In addition, it has all the needed decoupling capacitors and power line for proper operation of the sensor. It is usable for the DIL24 socket and adaptable with an STEVAL-MK137V1 motherboard.

The communication started in configuring only one sensor for understanding the working principle and continued on adapting SPI interface. The electrical connection of the sensor was used according to the datasheet also shown below in figure 13. Due to unknown reasons; the sensor could not function as expected. As a result, it was necessary to change the sensor because of hardware failure expectations but the second sensor showed the same result. I2C interfacing has also been adapted to test the operation of LIS3MDL nevertheless the sensor could not pass the self-test.

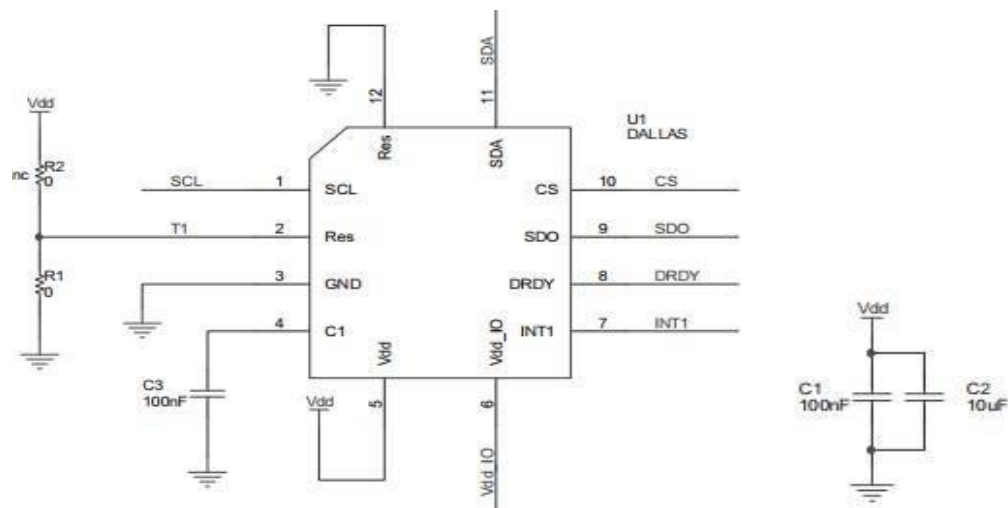


Figure 13. Schematics of STEVAL-MKI137V1 (Copied from STMicroelectronics, STEVAL-MKI137V1 LIS3MDL adapter board [16]).

Thus, LIS3MDL adapter board solved the entire problem and the system was able to pass the self-test and create communication between the sensor and microcontroller. The STMicroelectronics adapter board application note has a precise electrical connection with unambiguous pin arrangement.

### 4.3 Analog Front End

It is a circuitry that consists of OPAMPs, filters, ASIC and other necessary electronic functional blocks to interface different sensors to ADC or microcontroller. ADS1296 is one of Texas Instrument's AFE (analog front end) used in the health monitoring. It has been used to interface the sensors with a microcontroller, the central unit which control sensors data storage and communications.

#### 4.3.1 ADS1296

This is a multichannel, low power ADC with built in PGA, internal reference and onboard oscillator giving 24 bits of data output per channel in binary twos complement with MSB first.

The data rate of the ADC in ADS1296 extends from 250 SPS to 32 kSPS. It has four GPIO pins for general use allowing the digital I/O pins to be individually configurable as either input or output in GPIO register. Communication is through SPI interface. ADS1296 contain on-chip temperature sensor which was not used in this project though it can be configured accordingly for a specific application. The ADC in ADS1296 can measure up to 6 differential voltages with the ability to display 6 channels and this was one important reason to select the ADC in the ADS1296 and higher data output rate for better resolution.

#### 4.3.2 Operation Principle

To read the analog data from the sensors, the ADC in ADS1296 is an important electronics system. The ADC converts analog data to digital data because of the microcontroller processors ability to read only digital data, i.e. 1s and 0s.

The processor in the microcontroller is not able to do anything with the Analog data that may be sent to it by a device. In order to read the data, the ADC is responsible in changing analog data to digital data. There are four SPI interface signal pins to build communication between the ADC and microcontroller: CS (chip select), SCLK (Serial clock), DIN (Data IN) and DOUT (Data OUT). The chip select, as the name describes, selects the chip for SPI communication and stays low until the end of the communication.

It is always advisable to hold the chip select for four or more clock cycles before taking it back to high. The serial clock (SCLK) is useful for transmission of command and data from the ADS. Once chip select is low, the device starts to execute the command every eight serial clocks.

The data input including the SCLK is used to communicate with the ADS and the data out (DOUT) with the SCLK which is the serial clock is used to register and read data from the ADS.

### 4.3.3 Interfacing ADS1296

The analog digital converter in ADS1296 gives data rates ranging from 250 SPS to 32 kSPS. Texas instruments ADS1296 has four general purpose GPIO pins and SPI configuration were adopted for communication.

As stated earlier in the introduction of ADS1296, it produces output data of twos complement form with 24 bits of data for each channel allowing the most significant bit to be the first data out. SPI configuration helps in writing, reading, converting and controlling data. The other important pin is DRDY (Data Ready) pin that points when data is ready. To understand the operation of this GPIO pins, let's look at figure 19 below.

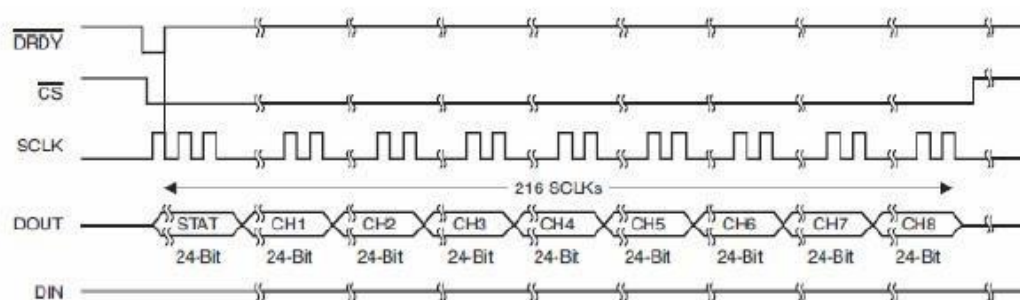


Figure 14.SPI Bus data Output for ADS1298 (Copied from Texas Instruments [18]).

In the operation of the ADS, the DRDY (data ready) goes low means ready data exists and shifted out on the rising edge of SCLK (clock) also because of continuous conversion mode configuration for this project, it shows when data is available. From figure 14, it is understandable that the CS (chip select) selects the ADS for communication. When CS goes low, communication starts and stays low until the end of the communication. The SPI initialization has been configured in the manner of the ADS CLK and ADS MISO as output and ADS MISO as input moreover pull up resistor were initialized. The DOUT (data out) line shows the status register value and output data for selected channels. The ADS1296 used in this project has 6 channels which means data out line shows status register value and data out for six channels.

The data transmission follows MSB first, Master mode, Synchronous 3 wire SPI, ACLK clock source and data is captured on the first UCLK edge and change on the following edge.

```
//=====
CS_PORT_OUT &= ~(CS_ADC);
ADC_RW(WREG_BASE+CONFIG2_ADDR);
ADC_RW(0);
ADC_RW(0x10);
CS_PORT_OUT |= CS_ADC;
__delay_cycles(1000);
//=====
```

Figure 15. Opcodes and command

Opcodes (operational codes) are used to configure and send commands of the ADS. Figure 15 shows an opcode with an address 0x02 CONFIG2 (configuration register) and the number of registers to read and write.

#### 4.4 Microcontroller: MSP430

It is an embedded system consisting of programmable peripherals, memory and processor for various applications for example: phones, automobiles, machines, medical devices and other embedded systems. Microcontrollers differ in their type; bits, flash size, RAM size, speed, supply voltage and a number of input/output lines categorize MCUs in different types. Programmable microcontroller's conception is to use it in embedded application which is being used widely and in this project.

##### 4.4.1 Operation Principle and Modes

The Texas Instruments MSP430FR5724 ultra low power microcontroller has been used while working on this project. It features ultra-low power 16-bit MSP430 CPU, nonvolatile memory, 10-bit A/D converter, 16 channel comparator, serial channel allowing SPI, I2C and UART protocol, real-time clock and other peripheral for different applications. MSP430 has one active mode and configurable low power modes LPM0, LPM1, LPM2, LPM3 and LPM4.

Once an interrupt happens, the device will exit from low power mode and perform its normal operation and again go back to LPM. The LPMs are necessary and designed to achieve: ultra-low power, decrease current consumption and speed and data throughput which were the main aim in working on knee angle measurement project. The configuration of these power modes is through CPUOFF, OSCOFF, SCG0 and SCG1 mode control bits that are found in SR (status register).



The microcontroller is the central unit in knee angle project. It acts as a bridge between the sensor and ADS and wireless module. The ADS transfers digitally converted data to the MCU for process and transmission to the nRF24L01.

#### 4.4.2 Clock System

The microcontroller consists of four system clock signals that allow selecting suitable performances and low power consumption. It comprises up to five clock sources and figure 16 states the configuration of clock source in relative to the desired performance and power consumption.

The low-frequency or high-frequency oscillator, internal low power low-frequency oscillator, internal digitally controlled oscillator (DCOCLK), optional high-frequency oscillator are the system clock signals for the microcontroller.

There are four system clock signals from the clock system module: ACLK (Auxiliary Clock) – is software selectable system clock signal. MCLK (Master clock) – is again software selectable which is used by the CPU and system. The last two are SMCLK (Subsystem Master Clock) and MODCK (Module Clock).

The DCOCLK; it is an integrated digitally controlled oscillator with three frequency selections also used as a source for ACLK, MCLK or SMCLK

```
CSCTL1 = DCOFSEL0 + DCOFSEL1;
CSCTL2 = SELA_3 + SELS_3 + SELM_3;
CSCTL3 = DIVA_0 + DIVS_0 + DIVM_0;
```

Figure 16. Control register configuration

The above stated Clock system control registers in figure 16 are used to set the DCO frequency range, ACLK and source divider which divides the frequency of the ACLK clock source. Figure 17 shows the configuration of the Control word register and eUSCI\_A clock source select (UCSSELx) bit to control the bit clock.



```
UCA0CTLW0 |=UCCKPH| UCMSB | UCMST | UCSYNC | UCMODE0 | UCSSEL_1;
UCA0CTLW0 |= UCSSEL_1;
```

Figure 17.Examples from the project to show configurations

The figure shows selection of data capture on the first CLK edge and change on the following edge, most significant bit data transfer, master mode selection in synchronous form of data transfer, 3-pin SPI mode and ACLK (auxiliary clock) eUSCI clock source selection.

#### 4.4.3 Enhanced Universal Serial Communication Interface - SPI Mode

This section describes the eUSCI\_A and eUSCI\_B configuration for serial communication in SPI. In SPI mode, the master feed shared clock for serial data communication between many devices. The eUSCI\_A initialization was configured to be used for the nRF24L01 wireless module whereas the eUSCI\_B for the ADS SPI initialization.

There are three or four signals we should count in while working on SPI mode.

- UCxSIMO: Slave In, Master Out
- UCxSOMI: Slave Out, Master In
- UCxCLK: eUSCI SPI Clock
- UCxSTE: Slave Transmit Enable, not used because of 3 wire SPI configuration for this project.

Example codes from figure 18 illustrate easily how to configure eUSCI in 3 pin SPI modes. The first line describes the initialization of eUSCI by setting UCSWRST bit that holds eUSCI in a reset condition. Modulation is not used for SPI mode which is shown in the second line of the code. The third line sets the main features of the SPI mode by choosing master mode (UCMST), setting the division factor of the eUSCI clock source (UCA0BR0), synchronous mode (UCSYN), most significant bit first controlling the direction of the transmit and receive register (UCMSB), eUSCI clock source select by UCSSEL\_\_ACLK which selects auxiliary clock source, phase selection of the clock (UCCKPH).Clearing the UCSWRST starts eUSCI for operation otherwise it stays in a reset mode until it is cleared.

```

UCA0CTLW0 = UCSWRST;
UCA0MCTLW = 0;
UCA0CTLW0 |= UCCKPH+ UCMSB + UCMST + UCSYNC+UCSSEL__ACLK ;
UCA0CTLW0 |= UCSSEL__ACLK ;
UCA0BR0 |= 0x02;
UCA0BR1 = 0;
UCA0CTL1 &= ~UCSWRST;

```

Figure 18. Example code of eUSCI configuration

The UCCKPH and UCCKPL in control word register are used to configure the polarity and phase of UCxCLK in eUSCI.

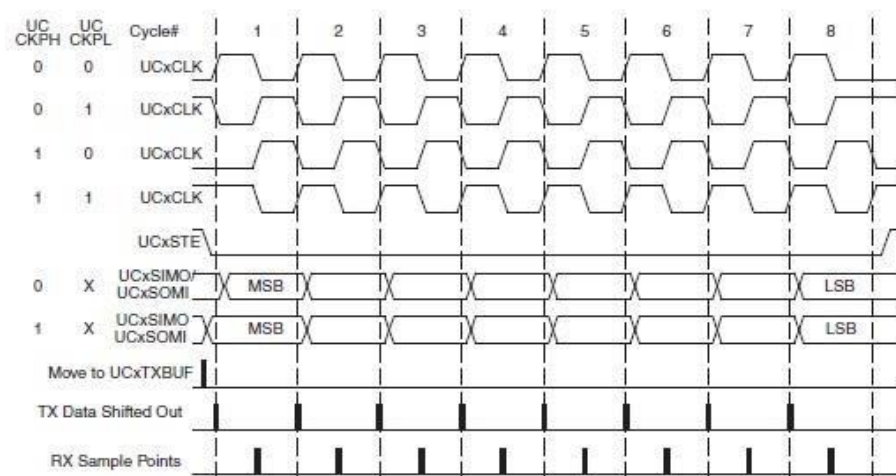


Figure 19. eUSCI SPI timing with UCMSB=1 (Copied from Texas Instruments, SLAU272 [19]).

The UCCKPH from eUSCI\_A control word zero registers is designed to describe the clock phase selection showing data capture on the first UCLK edge and change on the following edge. Looking at figure 19, we can understand the data is captured on the first UCLK edge with MSB (most significant bit) first.

#### 4.4.4 MSP-FET430UIF universal programmer

It is a universal programmer used to interface and program MSP430 series microcontrollers. MSP430F5xx and MSP430F6xx family use the 2-Wire JTAG communication (SPY-Bi-Wire). This universal programmer was used in debugging the programmed code and the electrical

connections to the microcontroller were easy due to the QFN2B designed chip by Thomas More University. Only TEST, RST, Vcc TOOL and GND as seen from figure 20 were connected to the TEST, RST, Vcc and GND of the microcontroller for debugging.

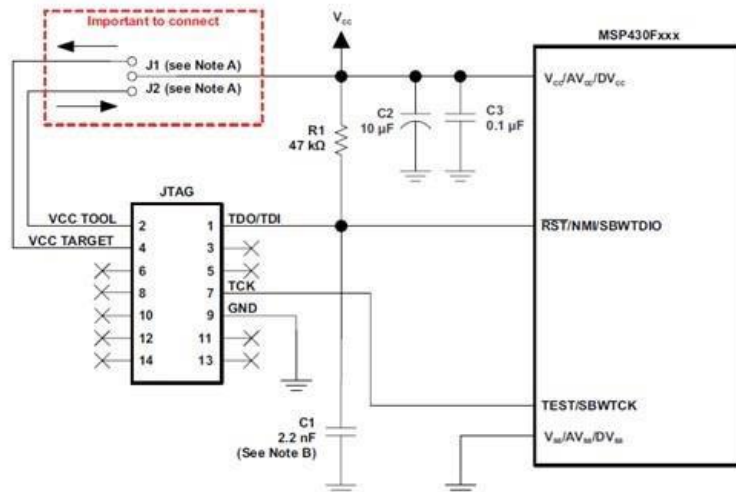


Figure 20. Connection guide for 2-Wire JTAG communication (Copied from Texas Instruments [20]).

The above figure shows the four useful pin connections to the microcontroller for debugging and appendix 2 shows the designed QFN24B pin configuration based on the microcontroller. The universal programmer can be seen in appendix 1 in connection to the test board.

#### 4.5 Wireless Module: nRF24L01

The nRF24L01 is a single chip 2.4 GHz transceiver with air data rate up to 2Mbps allowing an ultra-low power operation. It is used widely in many applications for example in sports watches and sensors, home and commercial automation, active RFID, others. The SPI configurable nRF24L01 is an easy wireless module due to its suitable configurable features.

##### 4.5.1 Features and Modes

The nRF24L01 needs six digital signals for data and control interfacing. The IRQ, CE, CSN, SCK, MOSI, MISO signals.

The IRQ is the interrupt signal pin used by three maskable interrupt sources and the CE (chip enable) is an active high signal pin to set the nRF24L01 to receiver and transmitter.

Table 2. Operational configuration modes for nRF24L01 (copied from Nordic Semiconductors, nRF24L01 Product Specification) [21, 21]

Mode	PWR UP register	PRIM RX register	CE	FIFO state
RX mode	1	1	1	-
TX mode	1	0	1	Data in TX FIFO. Will empty all levels in TX FIFO <sup>a</sup> .
TX mode	1	0	minimum 10 $\mu$ s high pulse	Data in TX FIFO. Will empty one level in TX FIFO <sup>b</sup> .
Standby-II	1	0	1	TX FIFO empty
Standby-I	1	-	0	No ongoing packet transmission
Power Down	0	-	-	-

In this operating mode if the CE is held high the TX FIFO is emptied and all necessary ACK and possible retransmits are carried out. The transmission continues as long as the TX FIFO is refilled. If the TX FIFO is empty when the CE is still high, nRF24L01 enters standby-II mode. In this mode the transmission of a packet is started as soon as the CSN is set high after an upload (UL) of a packet to TX FIFO. This operating mode pulses the CE high for at least 10 $\mu$ s. This allows one packet to be transmitted. This is the normal operating mode. After the packet is transmitted, the nRF24L01 enters standby-I mode. (Nordic Semiconductor, nRF24L01 product specification) [21, 21]

#### 4.5.2 Interfacing with nRF24L01

In interfacing the nRF24L01; Vcc, GND, IRQ, CE and four SPI bus pins CSN, SCK, MISO and MOSI are important. The four SPI interfacing pins are useful for data transmission and reception showing SPI full-duplex bus property which means sending and accepting data at once in different lines.

The CSN (chip-select not) is enable pin for the SPI, it is kept high unless SPI command is sent to the device to get data on the SPI bus from our microcontroller.

MOSI (Master Out Slave In) describes the microcontroller as master and nRF24L01 as a slave due to nRF24L01 always sending data only when there is a request from the microcontroller and the master send data to nRF24L01.

MISO (Master In Slave Out) the slave (nRF24L01) sends data according to the request from the master (Microcontroller). Once the nRF24L01 connection to the microcontroller is set, SPI interfacing is not a hard task.

Understanding the register instructions and format makes the operation easy. Each register has an address to write or read and other specific tasks.

The W\_register allows users to write to the registers in the nRF24L01. The received data packet is saved in RF\_FIFO in RX mode and R\_RX\_PAYLOAD is useful in checking a received packet in RX\_FIFO register. The W\_TX\_PAYLOAD is used while sending a packet in TX-mode; the first step is to send a command byte (A0) which starts the operation in TX-mode and continue with the payload. The most important thing to consider is to set the same payload for the sender and receiver to communicate. The CONFIG register is also the other important register to consider in starting the operation of nRF24L01. It consists of the PWR\_UP bit that should be set to make the nRF24L01 device work; PRIM\_RX bit in CONFIG register determines the device as receiver and transmitter, clearing this bit sets the device as transmitter and on the other way setting this bit sets the device as receiver.

#### 4.4.3 Transmitter and Receiver

This subsection discusses the transmitter and receiver mode of nRF24L01. The nRF24L01 enters to Rx-mode (receiver mode) while configuring the PWR\_UP bit and PRIM\_RX bit from CONFIG register to high. The CE (chip enable) also stays high to set the nRF24L01 to RX mode.

The RX-mode sets nRF24L01 to receiver mode. The configuration of RX-mode starts with setting the same address as to the transmitter for proper communication. Figure 21 shows TX address setting for nRF24L01 and the RX should be set in the same address setting for proper communication.

```
static BYTE TX_ADDRESS[5]={0x01,0x23,0x45,0x67,0x89};
```

Figure 21. Setting TX address

The auto acknowledgement bit for selected pipes has to be set in the EN\_AA register; the RF\_channel should also be set according to the frequency of the nRF24L01 operation mode. The RF frequency channel can be calculated using the formula below

$$F_0 = 2400 + \text{RF\_CH} \text{ [MHZ]} \quad (1)$$

The number of bytes in RX payload should be set in RX\_PW\_P0 (RX payload width data pipe0) as in the same manner and width to TX payload.

```

CE_LOW;
SPI_Write_Buf(WRITE_REG + RX_ADDR_P0, TX_ADDRESS, TX_ADR_WIDTH);

SPI_RW_Reg(WRITE_REG + EN_AA, 0x01);
SPI_RW_Reg(WRITE_REG + EN_RXADDR, 0x01);
SPI_RW_Reg(WRITE_REG + RF_CH, USED_RF_CH);
SPI_RW_Reg(WRITE_REG + RX_PW_P0, TX_PLOAD_WIDTH);
SPI_RW_Reg(WRITE_REG + RF_SETUP, 0x0E);
SPI_RW_Reg(WRITE_REG + CONFIG, 0x0f);

CE_HIGH;

```

Figure 22. nRF24L01 wireless module RX mode configuration

The SPI\_Write\_Buf line from figure 22 indicates setting RX address as the same as the TX device address. The EN\_AA register is used to set the auto acknowledgement bit and enable auto acknowledgment data pipe 0 the same with enable RX address pipe 0 were selected in this project. The RF\_CH register is used to set the RF channel frequency and the RF\_SETUP register is an important register in setting the air data rate with the value of 2Mbps and RF output power in TX mode as 0dBm. The last line (CE high) enables the RX device.

The receiver and transmitter should be set with the same air data rate for communication. The nRF24L01 offers 1Mbps and 2Mbps air data rate options. Choosing high air data rate gives lower average current consumption and due to this advantage 2Mbps was selected while working on the project. TX-mode as the name implies is the transmitter mode of the chip. The PWR\_UP bit is set high as the same as the RX-mode but the PRIM\_RX should be cleared to enter to TXmode. The TX FIFO payload should be set and importantly the CE (chip select) bit should stay high for more than 10µs. Table 2 describes an easy way to configure the TX and RX modes

```

CE_LOW;

SPI_Write_Buf(WRITE_REG + TX_ADDR, TX_ADDRESS, TX_ADR_WIDTH);
SPI_Write_Buf(WRITE_REG + RX_ADDR_P0, TX_ADDRESS, TX_ADR_WIDTH);
//SPI_Write_Buf(WR TX_PLOAD, tx_buf, TX_PLOAD_WIDTH);
SPI_RW_Reg(WRITE_REG + EN_AA, 0x01);
SPI_RW_Reg(WRITE_REG + EN_RXADDR, 0x01);
//SPI_RW_Reg(WRITE_REG + SETUP_RETR, 0x1a);
SPI_RW_Reg(WRITE_REG + SETUP_RETR, 0x0a);
SPI_RW_Reg(WRITE_REG + RF_CH, USED_RF_CH);
SPI_RW_Reg(WRITE_REG + RF_SETUP, 0x0C);
SPI_RW_Reg(WRITE_REG + CONFIG, 0x0e);

```

Figure 23. nRF24L01 wireless module TX mode configuration



Figure 23 shows SPI configuration for TX mode of nRF24L01. The first line writes the TX\_Address to nRF24L01 and enables auto acknowledgment pipe0 with auto retransmit delay of 250us. The CONFIG register sets the PWR\_UP bit and enable the cycle redundancy check (CRC detects error in data packets) to 2 bytes. TX and RX modes have common configuration features for proper communication. Setting the address, auto acknowledgement, RF channel, payload width, RF transmit power and data rate, retransmit settings have to have the same configuration setting and most importantly extra attention to the CONFIG register configuration of nRF24L01.

## 5 Comparison

This section compares the systems and devices used in knee angle measurement project. The project focused on advancing the system for better performance by comparing and drawing solutions.

### 5.1 Design and Units

This subsection covers design comparison between the old and new schematic design and PCB. Figure 24 shows the old designed schematic board and figure 25 shows the new designed schematic board designed by Jurre De Weerd at Thomas More University.

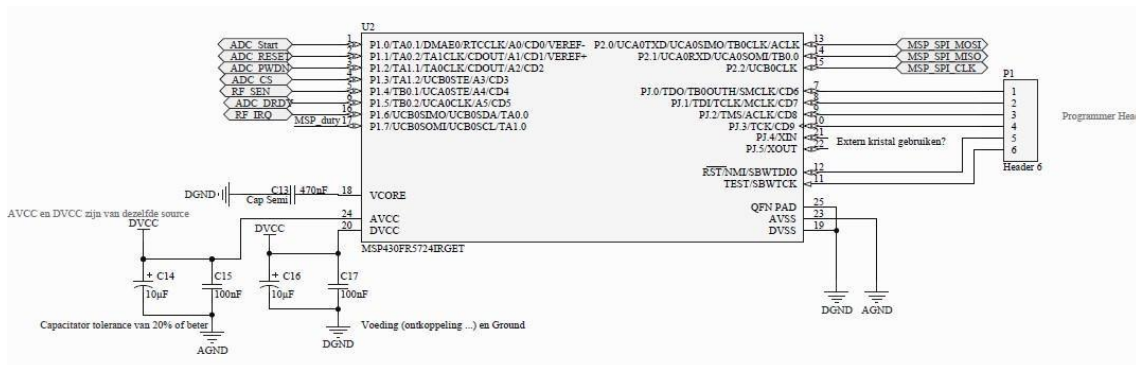


Figure 24. Old designed schematic (Copied from EMSYS, Campus De Nayer by Jurre De Weerd)





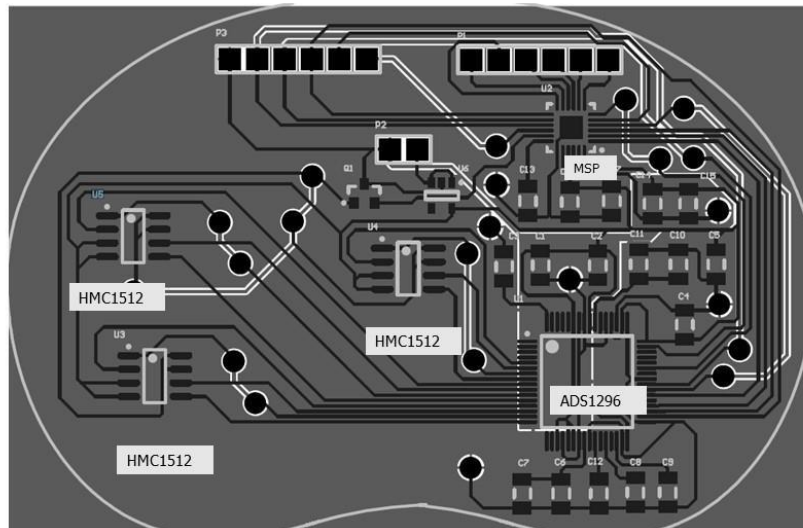
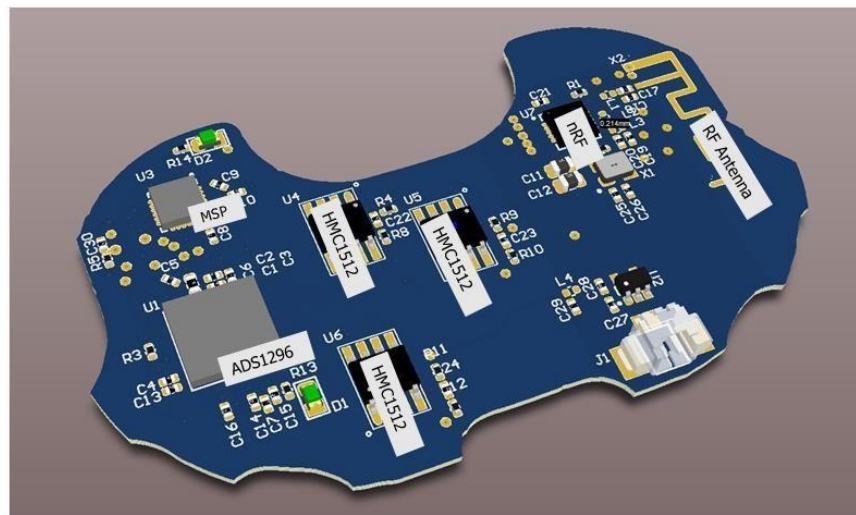


Figure 26. Old PCB design (Copied from EMSYS, Campus De Nayer by Jurre De Weerd)

The old printed circuit board was replaced by new printed circuit board one for the advantage of placing the wireless module in the same board with the other systems. Figure 27 shows the new designed printed circuit board with three HMC1512 sensors, analog front end (ADS1296), microcontroller and especially the wireless module on the same printed circuit board. The other point to consider is that the new board has a smaller size compared to the old board.



Software comparison of the system focuses on SPI adoption of hardware and software interface. The first work was done in adopting software SPI for the system. Through the process, changes have been made for example converting the code flow of the software based SPI to understandable and easy code flow with descriptions. The work continued with adopting hardware SPI for the system that can handle the data transfer automatically.

## 5.2 Power Consumption

Low power mode is an advantage to save the current consumption in the process. The previous work done by one of the student in Thomas More University did not adopt interrupt and LPM (low power mode) so that it was one idea to use interrupts and low power mode to reduce current consumption in order to allow the system to rest while doing nothing and go back to normal operation mode when interrupt happens.

Code composer studio has two ways of code building options which is called Configurations. The first one is debug configuration, unoptimized way of debugging that maintains the symbolic debug configuration and secondly release (optimized) configuration. Released configuration adds options to transform the codes to release mode to make it easier to evaluate the performance of the optimized code. This feature can be adapted easily through code composer studio build options.

## 6 Testing Devices and Results

This section covers the devices used while testing the system and results. All the results are based on the test performed.

### 6.1 Saleae Logic Analyzer

It allows user to examine digital signals in electronic projects. This logic analyzer is easy to use and inexpensive. By plugging the logic analyzer to a computer user can visualize the digital signals in SPI, I2C, Serial, I-wire and other digital protocols.

The SPI for saleae logic analyzer has four main lines: Clock line, an enable line, master to slave line and slave to master line. The SPI setting can be adjusted in the right corner of the logic display.

The clock polarity (CPOL) and clock phase (CPHA) are one of the most important factors in outputting proper signal describing data validity in the clock leading edge or trailing edge.

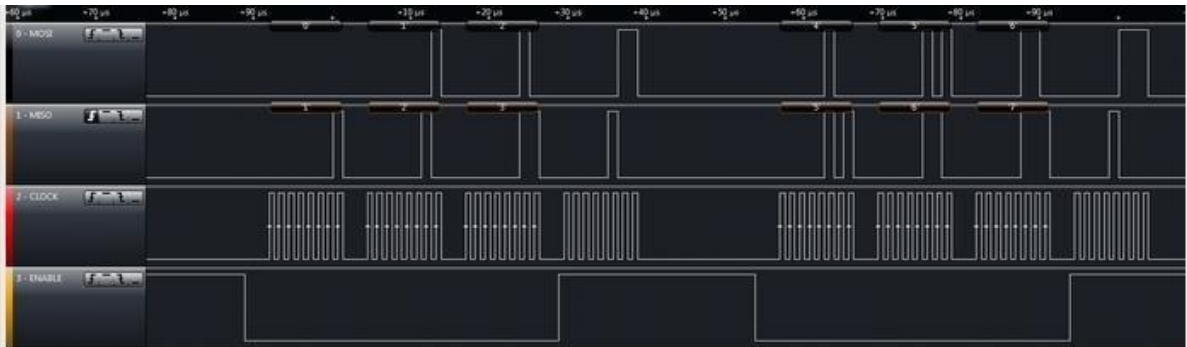


Figure 28. Saleae logic decodes of SPI (Copied from Saleae [22]).

Figure 28 shows how the saleae logic analyzer display looks like for SPI. It consists of the EN (enable) or the Slave Select (SS) acts as disabled when 1 and enabled when 0. MOSI is the master out slave in line showing the master holding the data output (MSB first). MISO (master in slave out) line shows the master holding the data input line (MSB first) and CLK is the clock line used by both MOSI and MISO.

This subsection discusses the visualized results from the ADS, nRF24L01 and lastly the LIS3MDL sensor communication with the whole system.

Figure 29 below shows the nRF24L01 saleae logic result indicating the STATUS register test result while checking the proper functionality of the wireless module. The 0x2E hexadecimal format from figure 29 logic display shows value of the STATUS register in the nRF24L01. The TX\_DS pin from the STATUS register is asserted when data is transmitted on TX. In order to start proper communication, it is advisable to clear this bit and MAX\_RT (maximum number of TX retransmit interrupt) again from the STATUS register to allow further communication.

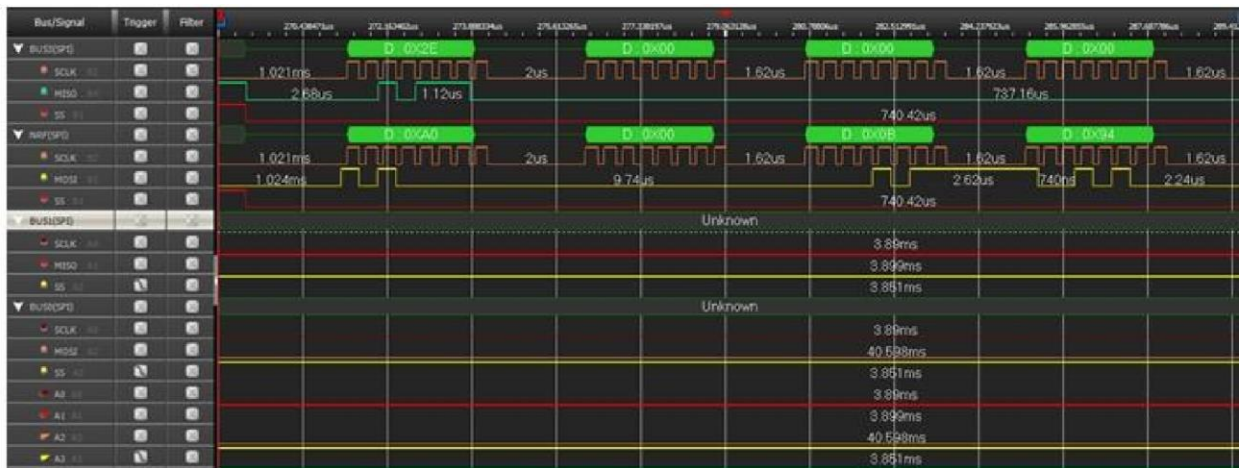


Figure 29. Saleae Logic analyzer results for nRF24L01 showing the status register in hexadecimal format every eight clock cycles and other dummy bytes.

The SS (Slave Select) or Enable pin goes low during communication and high at the end of communication. The NFR section from the display box shows the data from the nRF24L01 for every eight clock cycle in hexadecimal format again in the manner of most significant bit first. The other test measurement was carried out for ADS1296 to check proper result data. Figure 30 shows the data of the ADS1296 in hexadecimal format with most significant bit with 6 channel output data. The green boxes show the data from the ADS, the first hexadecimal value shows a dummy byte to show the communication is working properly and the other values show the data out for the six channels in hexadecimal data format for every eight clock cycles.

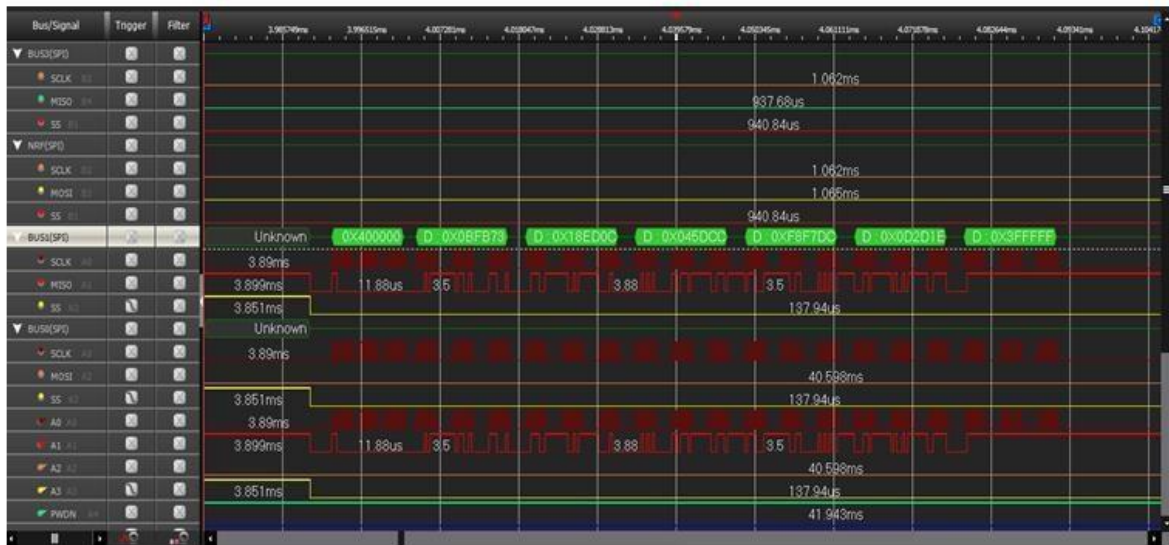


Figure 30. Saleae Logic analyzer result for ADS1296 indicating a dummy byte to show proper communication and six channel data in hexadecimal data format

The SS shows the same characteristics, low during communication and back to high at the end of communication. The BUS1 (SPI1) logic display box shows 24 bits data from the ADS1296. Appendix 3 shows more saleae logic analyzer results from the system.

## 6.2 LabVIEW

LabVIEW is one of the important software available to complete from simple to complex applications in engineering field. This development environment uses various components that are applicable in measuring, testing and controlling applications. Thomas More University has developed LabVIEW testing environment for knee angle measurement. This testing environment (UART measurement data receiver) as shown on figure 31 has three display parts. The first front panel showing the name of the developer, COM port with tab to allow proper selection of COM ports, round shaped circle to check connection status, RAW input data display box to display the data received and another display box to show sorted data from channel one (CH1) to channel six (CH6).

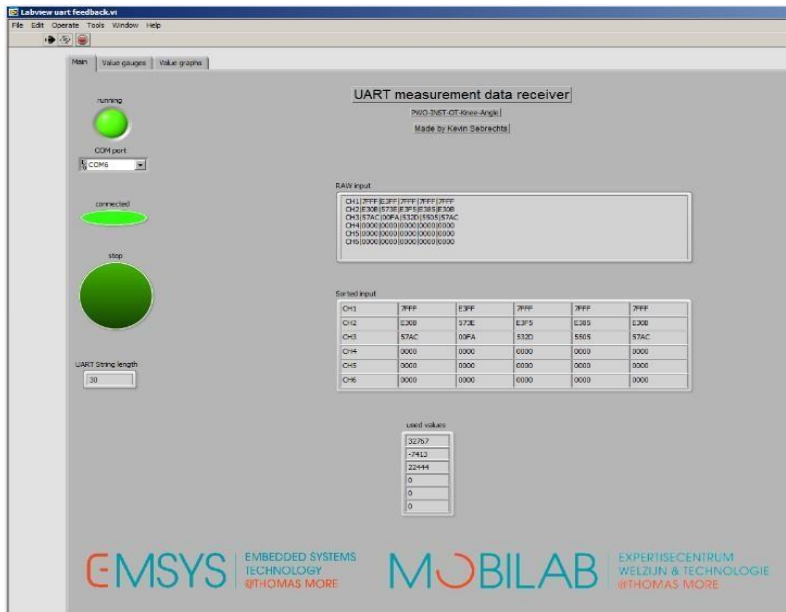


Figure 31. UART measurement data receiver main front panel (Thomas More University by Kevin Sebrechts)

The second front panel shows value gauges of the measurement system. Figure 32 indicates the change in gauge of the three sensors but in this test only one sensor was configured for testing so the XY orientation of sensor 1X and sensor 1Y is applicable.

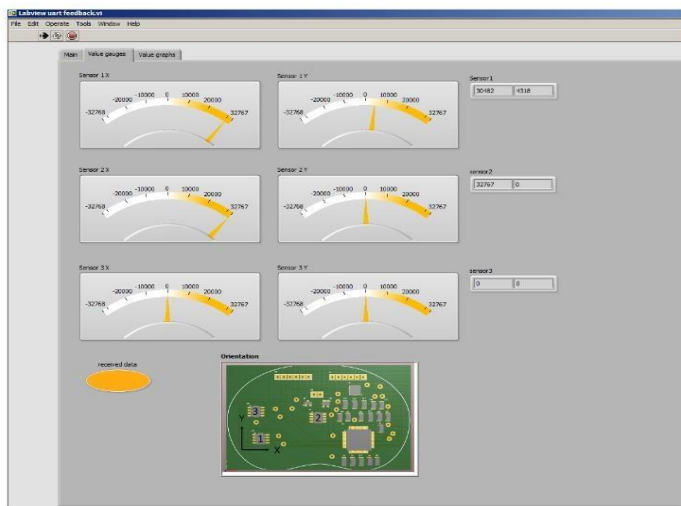


Figure 32. UART measurement data receiver value gauge front panel (Thomas More University by Kevin Sebrechts)



The third UART measurement data receiver panel is the value graph displaying the sensor value chart and sensor value graph. Both the chart and value graph shows change in values and shape while a magnet is closer or far away from the sensor. Putting the magnet closer increases the amplitude on both graphs.

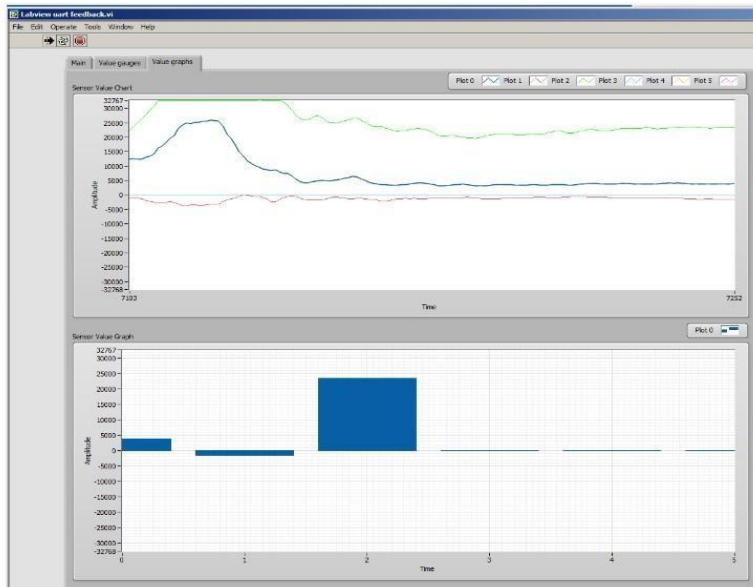


Figure 33. LabVIEW result of the LIS3MDL sensor and Magnet. It shows the change in amplitude only for one sensor in XYZ axis.

The aim of this test was to be able to get stable changes in sensor value chart and sensor value graph while the magnet is closer to the sensors or far away from the sensor. Figure 33 shows LabVIEW result of the system. According to the full scale measurement setup, the graph on figure 33 shows the change in amplitude according to the strength of the magnetic field. The graph shows change in magnetic field for XYZ axis. Only one sensor were adopted for communication so the graph displays the change in amplitude for one sensor in XYZ axis each line representing the X, Y and Z axis. Appendix 5 shows more LabVIEW results indicating stable amplitude change depending on proximity of a magnet.

### 6.3 MCP2200 (USB 2.0 to UART Protocol Converter with GPIO)

The MCP2200 is a USB to UART converter with GPIO that enables closer study of electronics projects and other applications. The UART interface has TX (Transmitter) and Receiver (RX) data signals to be connected to RX and TX of the device under test. The UART in this project was configured for 9600 baud rate and Real Term was used to display the data in hexadecimal data format.

The ready-made MCP2200 board from Thomas More University has Vcc, GND, RX and TX pin to connect to the microcontroller for proper data transmission and testing. The measurement test was performed in different Gauss level for LIS3MDL with given gain at 16-bit.

Refer to table 1 under LIS3MDL digital output magnetic sensor subsection to see different Gauss level for 16-bit. 4 gauss, 12 gauss and 16 gauss levels were selected under four different setups with and without magnet to study this measurement. The calculation of the milligauss and average gauss level were performed by changing the measured hexadecimal data to decimal data format and following the specific gain level and dividing by 1000 for milligauss level.

$$\text{milliGauss} = (\text{Sample value in decimal}) \div (\text{gain value for specific fullscale} \times 1000) \quad (2)$$

$$\text{Averagegauss} = (\text{Addition of sample values in milligauss}) \div (\text{number of samples}) \quad (3)$$

#### 6.3.1 Real Term

Real term is a serial terminal designed to capture, control, debug and display output data in binary or other complex data formats. It supports various configurations like SPI, I2C, 1Wire chip control and others. The setting can be adjusted to users need and data can be displayed in any of the formats listed on figure 34 below in Display As dialog box.

The baud rate relays on specific hardware ports. Once data is captured it is possible to save it as hexadecimal data format. Adding the timestamp and delimiter will give received data separated in time and comma or space depending on user selection.





Figure 34: Display Format of Real Term (Copied from Real Term Sourceforge [24]).

Real term was used in testing LIS3MDL sensor so that it is possible to study the performance of the sensor and the magnet. The distance between the sensor and the magnet was measured to see the difference in the gauss level. Using Real Term, the displayed hexadecimal data used to calculate the magnetic field in gauss. Appendix 4 page one and two shows the four different magnet position setups used to measure the sensor performance. The results of the sensor was logged in excel as shown in appendix 4 of page 3 to be able to calculate the sample results in decimal data format and milligauss based on formula 2 . Note that, the result from the Real Term is in hexadecimal format.

The average gauss can be calculated using formula 3 for XYZ axis. Using excel the result data was also shown in graphical representation as shown in the last page of appendix 4. Depending on the datasheet of LIS3MDI sensor the sensitivity describes the gain of the sensor which can be determined by applying a magnet field of a specific gauss to the sensor. Considering page 3 of appendix 4, the XYZ axis of the sensor without magnet shows deviation of an output signal from the ideal output and setup 2, 3 and 4 with magnet applied at 4 gauss shows an overflow due to gauss level over 4000 millogauss.

## 7 Conclusion and Discussion

The thesis explains the development of knee angle measurement consisting of various systems; sensors, analog front end, microcontroller and wireless module. Various development tools and software has been used while working on knee angle measurement for example LabVIEW, code composer studio, saleae logic analyzer, real term, excel, MCP2200 configuration utility, oscilloscope and other applications. Due to unknown reason, this electrical connection was not able to operate properly even though the soldering of the external capacitors was done twice for checking. As a result, LIS3MDL adapter board (STEVAL-MKI137V1) was replaced to solve the problem.

The ADS showed incomplete data functionality with the inability of proper ADS initialization. Timing problem is the expected cause. The wireless module presented complete performance of the chip. The RF antenna, the SPI configuration, receiver and timing showed meaningful results.

The difficulties in designed schematics and PCB board were solved by swapping and rearranging specific ports. The system can be improved by replacing CC430, an ultra-low power microcontroller system with integrated RF module. Moreover, eliminating the ADS to save up power consumption and reduce the printed circuit board will add up more advantages to the system.

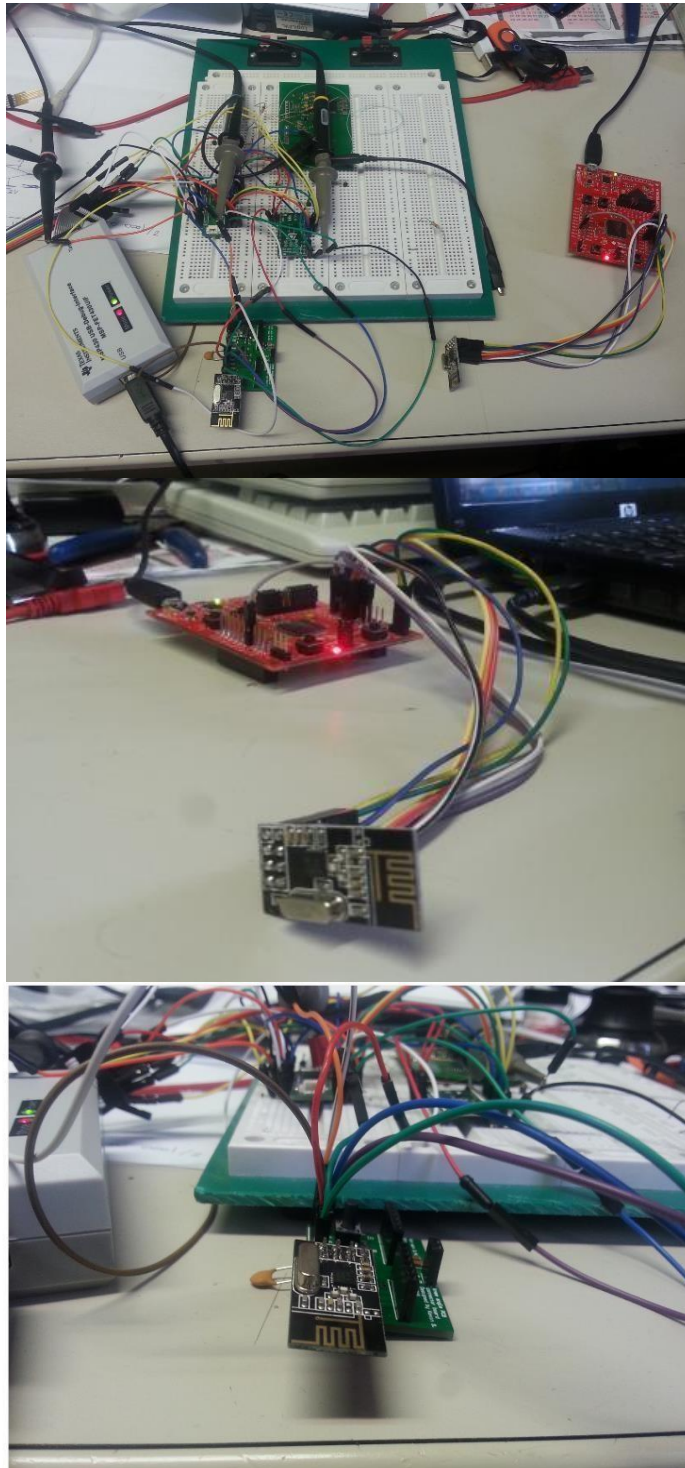
It can be concluded that the aim of the project was met in presenting the readable and descriptive code flow, upgrading the system to LIS3MDL sensors for better performance and most importantly, presenting stable output data and channel depending on the position and distance of the magnet.

## References

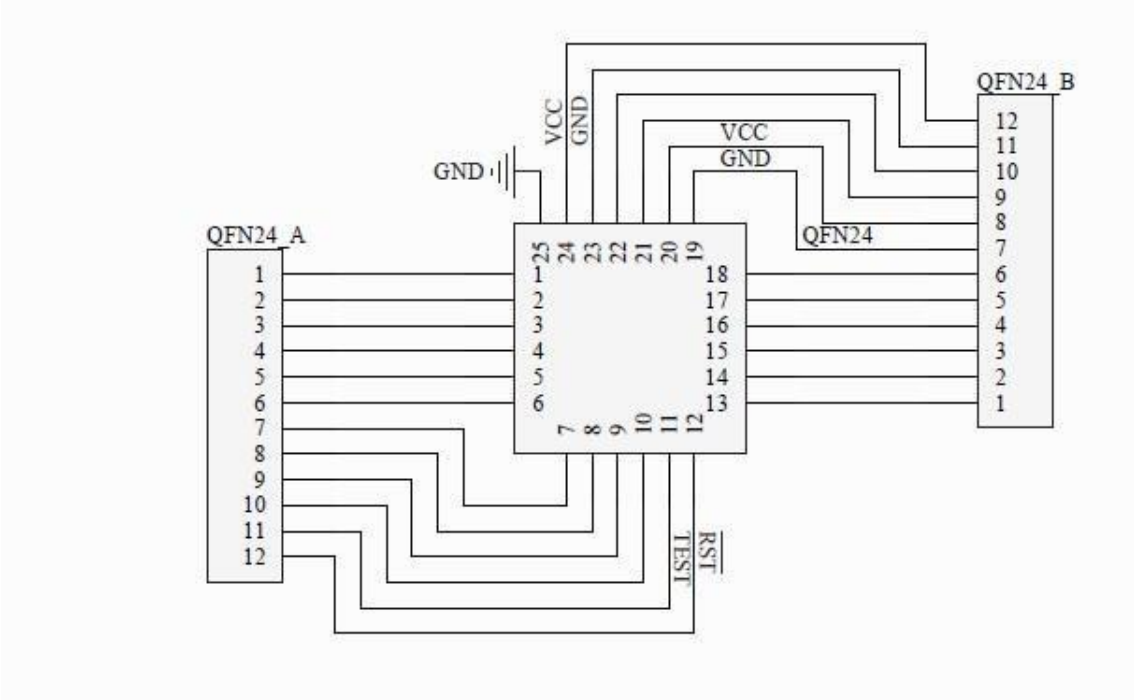
- 1 DR. RICHARD P.B.VON BORMANN. [Online].  
<http://www.capetownkneesurgery.co.za/knee-surgery-cape-town.php>  
[Accessed 25 July 2015]
- 2 "Tomi's Physio therapy Blog", Knee Injuries [Online].  
[http://thomasbondphysio.blogspot.fi/2014\\_09\\_02\\_archive.html](http://thomasbondphysio.blogspot.fi/2014_09_02_archive.html)  
[Accessed 10 August 2015]
- 3 AESCULAP, Implants Systems, Type of Knee Implants, Knee Design.  
[Online]. <https://www.soactivesofast.com/knee/types-of-knee-implants>.  
[Accessed 10 August 2015]
- 4 Knee Angle Measurement thesis documentation by Kevin Sebrechts and Sven Sleeckx, Thomas More University.
- 5 Arash ARAMI, Kinematics Estimation and Loosening Detection in Smart Knee Prostheses; Suisse 2014
- 6 A.Arami, A.Vallet and K.Aminian.Accurate Measurement of Concurrent Flexion-Extension and Internal External Rotations in Smart Knee Prostheses, in IEEE Transactions on Biomedical Engineering (TBME), 2013
- 7 Arash Arami, Hooman Dejnabadi, Vincent Leclercq and Kamiar Aminian. An Implantable System for Angles Measurement in Prosthetic Knee. International Society of Biomechanics (ISB), Brussels, Belgium 2011.
- 8 Chronic diseases and health promotion. [Online].  
<http://www.who.int/chp/topics/rheumatic/en/> [Accessed 10 August 2015]
- 9 A.Arami, M.Simonici, O.Atasoy, W.Hasenkamp and S.Ali et al. Instrumented Knee Prosthesis for Force and Kinematics Measurements, in IEEE Transactions on Automation Science and Engineering, 2013.
- 10 "supermagnete", S-05-08-N , Rod magnet.[Online]  
[http://www.supermagnete.de/eng/rod-magnets-neodymium/rod-magnetdiameter-5mm-height-8.47mm-neodymium-n45-nickel-plated\\_S-05-08-N](http://www.supermagnete.de/eng/rod-magnets-neodymium/rod-magnetdiameter-5mm-height-8.47mm-neodymium-n45-nickel-plated_S-05-08-N). [Accessed 10 August 2015 ]
- 11 KOHDEN, Principle of the AMR sensor. [Online].  
[http://www.hkd.co.jp/english/amr\\_tec\\_amr/](http://www.hkd.co.jp/english/amr_tec_amr/) [Accessed 13 August 2015]
- 12 "Honeywell" Magnetic Displacement Sensors, HMC1501/1512 datasheet. [Online.] <http://www.farnell.com/datasheets/1681861.pdf>. [Accessed 20 August 2015]

- 13 STMicroelectronics, LIS3MDL datasheet-production data. [Online].  
<http://www.st.com/st-webui/static/active/en/resource/technical/document/datasheet/DM00075867.pdf>  
[Accessed 20 August 2015]
- 14 STMicroelectronics, LIS3MDL Application Note. [Online].  
[http://www.st.com/st-webui/static/active/cn/resource/technical/document/application\\_note/DM00136626.pdf](http://www.st.com/st-webui/static/active/cn/resource/technical/document/application_note/DM00136626.pdf). [Accessed 20 August 2015]
- 15 STMicroelectronics, STEVAL-MKI137V1 LIS3MDL adapter board for standard DIL24 socket datasheet.[Online]  
[http://www.st.com/st-webui/static/active/en/resource/technical/document/data\\_brief/DM00089855.pdf](http://www.st.com/st-webui/static/active/en/resource/technical/document/data_brief/DM00089855.pdf). [Accessed 22 August 2015]
- 16 STARS; Sensors Technology Applied In Reconfigurable Systems; Analog Front Ends. [Online].  
<http://starsproject.nl/activities/theme2/> [Accessed 13 August 2015]
- 17 "Texas Instruments", ADS1296 Analog to Digital Converter with Integrated ECG Front End. [Online].  
<http://www.ti.com/lit/ds/symlink/ads1296.pdf> [Accessed 13 August 2015]
- 18 "Texas Instruments", SLAU272; MSP430FR57xx Family User Guide. [Online].  
<http://www.ti.com/lit/ug/slau272c/slau272c.pdf>. [Accessed 17 August 2015]
- 19 "Texas Instruments", MSP-FET430UIF universal programmer, MSP430 hardware tool.  
<http://www.ti.com/lit/ug/slau278v/slau278v.pdf>. [Accessed 17 August 2015]
- 20 "Nordic Semiconductors", nRF24L01 product specification. [Online].  
<http://www.nordicsemi.com/eng/Products/2.4GHz-RF/nRF24L01>. [Accessed 20 August 2015]
- 21 Saleae Logic Analyzer. [Online].  
<https://www.saleae.com/index>. [Accessed 20 August 2015]
- 22 "Microchip", MCP2200 USB 2.0 to UART Protocol Converter with GPIO. [Online].  
<http://ww1.microchip.com/downloads/en/DeviceDoc/22228B.pdf>. [Accessed 20 August 2015]
- 23 Realterm: Serial Terminal.[Online].  
<http://realterm.sourceforge.net/> [Accessed 08 September 2015]

### Measurement Setup including Transmitter and Receiver



**QFN Package design for the Microcontroller (Created by Kevin Sabrechts, Thomas More University)**

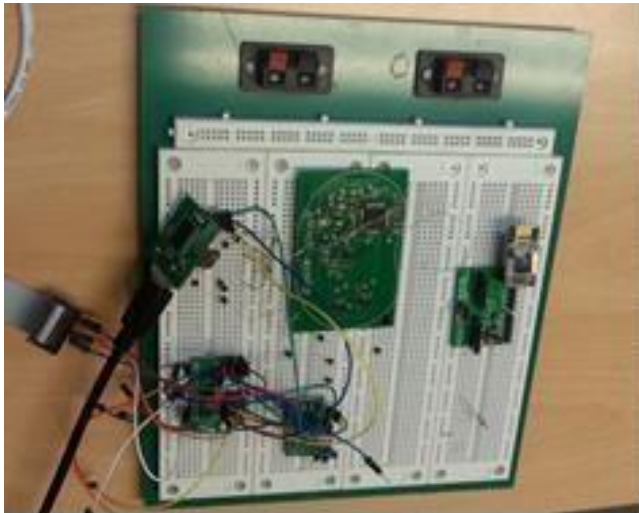




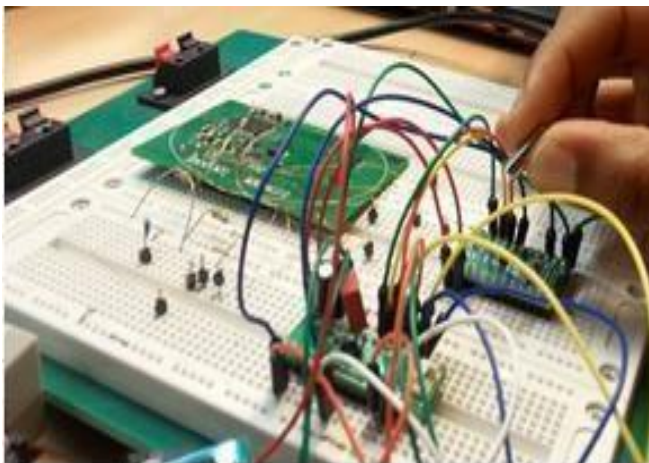
## Saleae Logic Analyzer test results



**Four different magnet position setups**



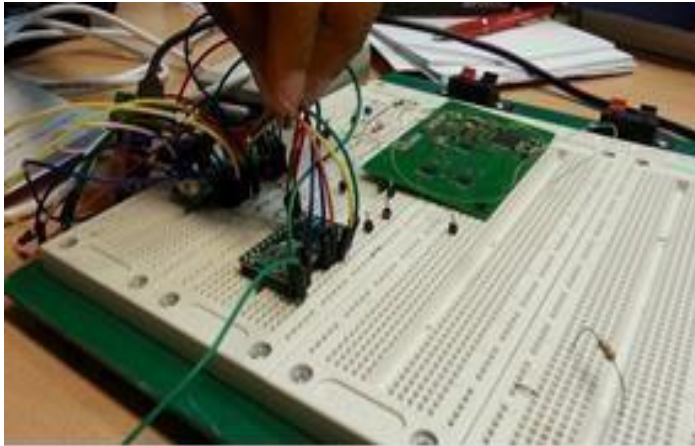
**SET UP 1**



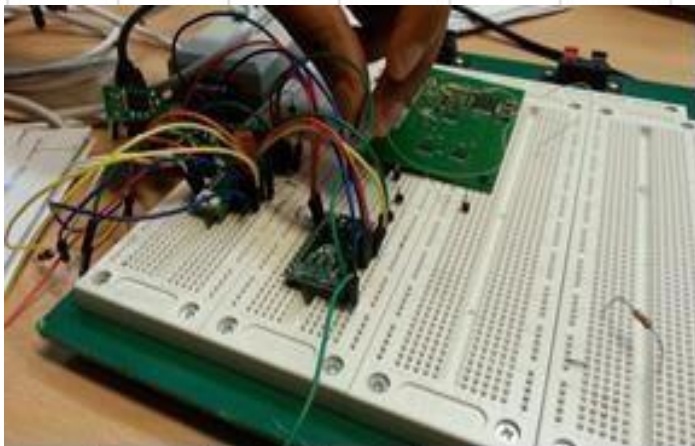
**SET UP 2**



Four different magnet position setups



SET UP 3



SET UP 4



**Magnetic data taken at 4 GAUSS for 12 samples**

**MAGNETIC DATA AT 4 GAUSS FULL SCALE WITH NO MAGNET APPLIED SET UP 1**

		sample 1	sample 2	sample 3	sample 4	sample 5	sample 6	sample 7	sample 8	sample 9	sample 10	sample 11	sample 12	AVERAGE
X AXIS	IN HEX	0178	015E	0179	0182	017E	014F	0179	0153	014A	014A	016C	0153	
	IN DECIMA	376	350	377	386	382	335	377	339	330	330	364	339	357,08
	IN mili GA	54,9547	51,1546	55,1008	56,4163	55,8316	48,9623	55,1008	49,5469	48,2315	48,2315	53,2008	49,5469	52,19
Y AXIS	IN HEX	0016	0035	002B	002E	0019	0030	0031	003C	0033	0033	0022	0031	
	IN DECIMA	22	53	43	46	25	48	49	60	51	51	34	49	44,25
	IN mili GA	3,2154	7,7463	6,2847	6,7232	3,6539	7,0155	7,1616	8,7694	7,4540	7,4540	4,9693	7,1616	6,47
Z AXIS	IN HEX	3155	3194	3176	3149	313D	3175	30F3	3156	3156	30EC	3127	310B	
	IN DECIMA	12629	12692	12662	12617	12605	12661	12531	12630	12630	12524	12583	12555	12609,92
	IN mili GA	1845,8053	1855,0132	1850,6285	1844,0514	1842,2976	1850,4823	1831,4820	1845,9515	1845,9515	1830,4589	1839,0821	1834,9898	1843,02

**MAGNETIC DATA AT 4 GAUSS FULL SCALE WITH MAGNET APPLIED SET UP 2**

		sample 1	sample 2	sample 3	sample 4	sample 5	sample 6	sample 7	sample 8	sample 9	sample 10	AVERAGE
X AXIS	IN HEX	4F69	4F8D	4F10	4E65	4E03	4E0F	4E36	4E82	4E3F	4DE6	
	IN DECIMA	20329	20365	20240	20069	19971	19983	20022	20098	20031	19942	20105,00
	IN mili GA	2971,2072	2976,4689	2958,1994	2933,2067	2918,8834	2920,6372	2926,3373	2937,4452	2927,6527	2914,6448	2938,47
Y AXIS	IN HEX	7FFF	7FFF	7FFF	7FFF	7FFF	7FFF	7FFF	7FFF	7FFF	7FFF	
	IN DECIMA	32767	32767	32767	32767	32767	32767	32767	32767	32767	32767	32767,00
	IN mili GA	4789,0968	4789,0968	4789,0968	4789,0968	4789,0968	4789,0968	4789,0968	4789,0968	4789,0968	4789,0968	4789,10
Z AXIS	IN HEX	8000	8000	8000	8000	8000	8000	8000	8000	8000	8000	
	IN DECIMA	-32768	-32768	-32768	-32768	-32768	-32768	-32768	-32768	-32768	-32768	-32768,00
	IN mili GA	-4789,2429	-4789,2429	-4789,2429	-4789,2429	-4789,2429	-4789,2429	-4789,2429	-4789,2429	-4789,2429	-4789,2429	-4789,24

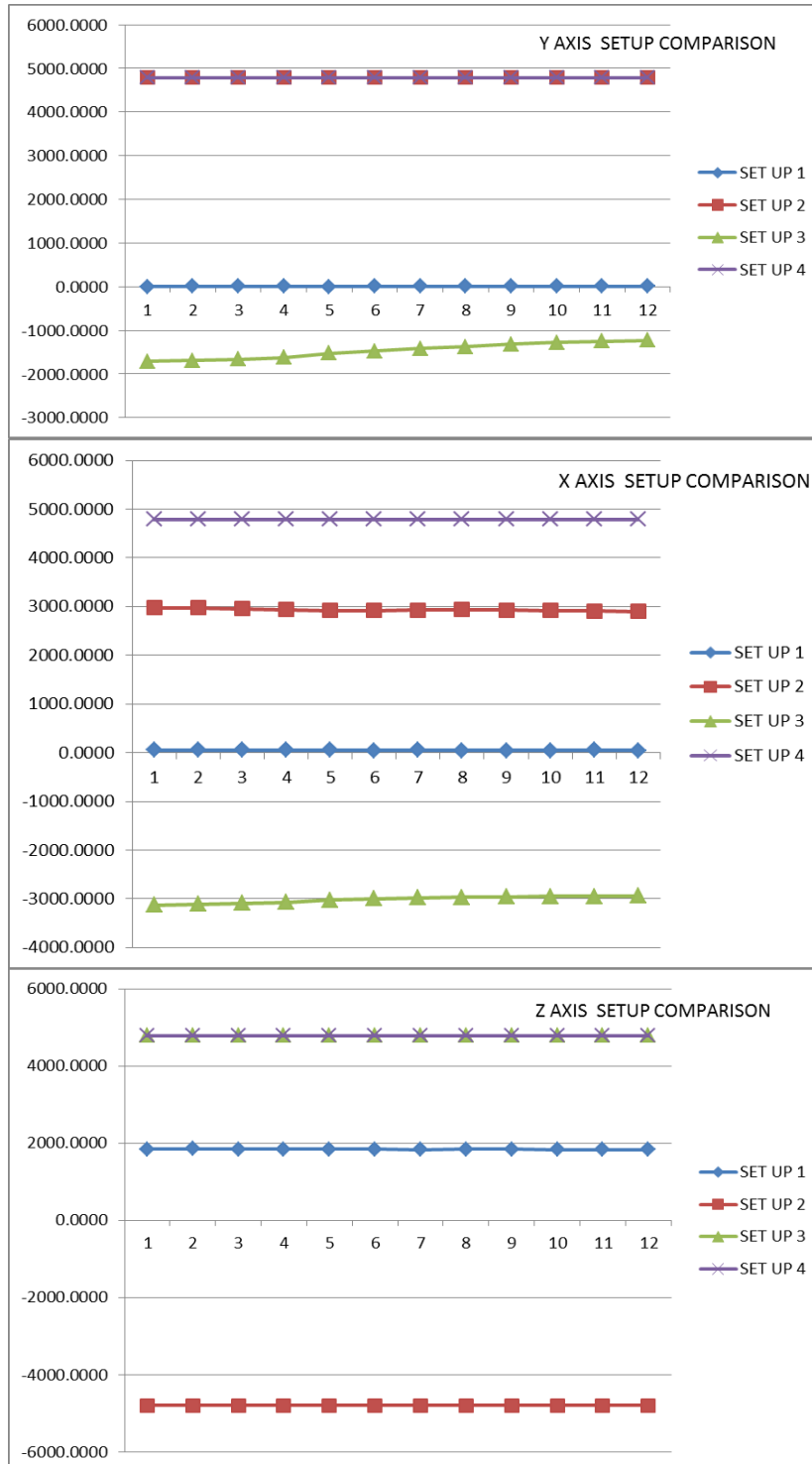
**MAGNETIC DATA AT 4 GAUSS FULL SCALE WITH MAGNET APPLIED SET UP 3**

		sample 1	sample 2	sample 3	sample 4	sample 5	sample 6	sample 7	sample 8	sample 9	sample 10	sample 11	sample 12	AVERAGE
X AXIS	IN HEX	AC7F	ACE4	AD53	ADE6	AF11	AFD1	B04F	B0AB	B0F9	B135	B133	B17D	
	IN DECIMA	-21377	-21276	-21165	-21018	-20719	-20527	-20401	-20309	-20231	-20171	-20173	-20099	-20622,17
	IN mili GA	-3124,3788	-3109,6171	-3093,3937	-3071,9088	-3028,2081	-3000,1462	-2981,7305	-2968,2841	-2956,8840	-2948,1146	-2948,4069	-2937,5913	-3014,06
Y AXIS	IN HEX	D22F	D2C3	D3A0	D4BE	D747	D8AD	DA0E	DB4D	DCD1	DDF2	DEB2	DF3B	
	IN DECIMA	-11729	-11581	-11360	-11074	-10425	-10067	-9714	-9395	-9007	-8718	-8526	-8389	-9998,75
	IN mili GA	-1714,2648	-1692,6337	-1660,3332	-1618,5326	-1523,6773	-1471,3534	-1419,7603	-1373,1365	-1316,4279	-1274,1888	-1246,1269	-1226,1035	-1461,38
Z AXIS	IN HEX	7FFF	7FFF	7FFF	7FFF	7FFF	7FFF	7FFF	7FFF	7FFF	7FFF	7FFF	7FFF	
	IN DECIMA	32767	32767	32767	32767	32767	32767	32767	32767	32767	32767	32767	32767	32767,00
	IN mili GA	4789,0968	4789,0968	4789,0968	4789,0968	4789,0968	4789,0968	4789,0968	4789,0968	4789,0968	4789,0968	4789,0968	4789,0968	4789,10

**MAGNETIC DATA AT 4 GAUSS FULL SCALE WITH MAGNET APPLIED SET UP 4**

		sample 1	sample 2	sample 3	sample 4	sample 5	sample 6	sample 7	sample 8	sample 9	sample 10	sample 11	sample 12	AVERAGE
X AXIS	IN HEX	7FFF	7FFF	7FFF	7FFF	7FFF	7FFF	7FFF	7FFF	7FFF	7FFF	7FFF	7FFF	
	IN DECIMA	32767	32767	32767	32767	32767	32767	32767	32767	32767	32767	32767	32767	32767,00
	IN mili GA	4789,0968	4789,0968	4789,0968	4789,0968	4789,0968	4789,0968	4789,0968	4789,0968	4789,0968	4789,0968	4789,0968	4789,0968	4789,10
Y AXIS	IN HEX	7FFF	7FFF	7FFF	7FFF	7FFF	7FFF	7FFF	7FFF	7FFF	7FFF	7FFF	7FFF	
	IN DECIMA	32767	32767	32767	32767	32767	32767	32767	32767	32767	32767	32767	32767	32767,00
	IN mili GA	4789,0968	4789,0968	4789,0968	4789,0968	4789,0968	4789,0968	4789,0968	4789,0968	4789,0968	4789,0968	4789,0968	4789,0968	4789,10
Z AXIS	IN HEX	7FFF	7FFF	7FFF	7FFF	7FFF	7FFF	7FFF	7FFF	7FFF	7FFF	7FFF	7FFF	
	IN DECIMA	32767	32767	32767	32767	32767	32767	32767	32767	32767	32767	32767	32767	32767,00
	IN mili GA	4789,0968	4789,0968	4789,0968	4789,0968	4789,0968	4789,0968	4789,0968	4789,0968	4789,0968	4789,0968	4789,0968	4789,0968	4789,10

Graphical representation of the four setups in XYZ axis



### Test result of the system from LabVIEW

